SUPPLEMENTAL MATERIALS AND METHODS

Competition Binding Assay

The immunoreactivities of BevF(ab')$_2$ and intact bevacizumab to VEGF were evaluated by a competition binding assay using ^{125}I-bevacizumab as the VEGF-specific radioligand. ^{125}I-bevacizumab was prepared by radiolabeling bevacizumab with Na^{125}I using the Iodogen method as previously described (1). Experiments were performed in VEGF-coated 96-well plates. These plates were prepared by incubating human recombinant VEGF 121 (5 μg/mL in bicarbonate buffer, pH = 9.0; M&C Gene Tech, Beijing, China) overnight at 4°C in high-binding 96-well Stripwell^{TM} enzyme-linked immunosorbent assay plates (100 μL per well, Costar, Cambridge, MA). The plates were washed and blocked with 10% fetal bovine serum (FBS). Afterwards, ^{125}I-bevacizumab (5.55 kBq) was added to the plates in the presence of increased concentrations of bevacizumab or BevF(ab')$_2$ (0 to 0.4 μM). After 2 h of reaction at room temperature, the plates were washed five times with phosphate-buffered saline (PBS). Each well was then wrested, collected in a tube, and measured in a γ-counter. The best-fit 50% inhibitory concentration (IC_{50}) values were calculated by fitting the data through nonlinear regression using Graph Pad Prism 4.0 (GraphPad Software, Inc.). Experiments were performed twice using quadruple samples.

Endothelial Cell Proliferation Assay

The 3-(4, 5-dimethylthiazolyl-2)-2, 5-diphenyltetrazolium bromide (MTT) assay

(2) was performed to measure the effect of gefitinib on the growth of endothelial cells. Human umbilical vein endothelial (HUVE) cells were isolated and cultured as previously described (3). HUVE cells (10^4 per well) were seeded in 96-well plates and incubated overnight to allow adherence. The cells were treated with various concentrations (0~50 μmol/L) of gefitinib for 72 h, and then 50 μL of MTT (1.0 mg/mL) were added to each well. After incubating at 37°C for 4 h, 100 μL of DMSO was added to each well and the plate was left in the dark for 2 h at room temperature. The absorbance at 570 nm was then measured using a plate reader. As a control experiment, MTT assay was also performed on 22B tumor cells (gefitinib-resistant) using the same procedures as described above. All experiments were performed with eight parallel samples and repeated twice.

Immunofluorescence Staining

Frozen tissue slices (5 μm thickness) were fixed with ice-cold acetone, rinsed with PBS, and then blocked with 10% FBS for 30 min at room temperature. For VEGF staining, the slices were incubated with FITC-bevacizumab (2 μg/mL) with or without a blocking dose of bevacizumab (20 μg) for 1 h at 37°C. After washing with PBS, the slices were visualized under a Leica TCS-NT confocal microscope (Wetzler, Heidelberg, Germany). For CD31 and Ki67 double staining, the tumor slices were incubated with rat anti-mouse CD31 (1:100; BD Biosciences, San Jose, CA) and rabbit anti-Ki67 (1:100; Chemicon, Millipore, Billerica, MA) antibodies. Visualization was then performed with FITC-conjugated goat anti-rat and

Cy3-conjugated donkey anti-rabbit secondary antibodies (1:200; Jackson Immuno-Research Laboratories, West Grove, PA) under the confocal microscope. After CD31 staining, 20 random views in the tumor slices were selected for microvascular density (MVD) analysis. MVD values were determined by counting and averaging the number of vessels with 20 fields of view.

References

1. Liu Z, Yu Z, He W, Ma S, Sun L, Wang F. In-vitro internalization and in-vivo tumor uptake of anti-EGFR monoclonal antibody LA22 in A549 lung cancer cells and animal model. *Cancer Biother Radiopharm.* 2009;24:15-24.

2. Niu G, Sun X, Cao Q, et al. Cetuximab-based immunotherapy and radioimmunotherapy of head and neck squamous cell carcinoma. *Clin Cancer Res.* 2010;16:2095-105.

3. Fu Y, Hou Y, Fu C, et al. A novel mechanism of gamma/delta T-lymphocyte and endothelial activation by shear stress: the role of ecto-ATP synthase beta chain. *Circ Res*. 2011;108:410-417.

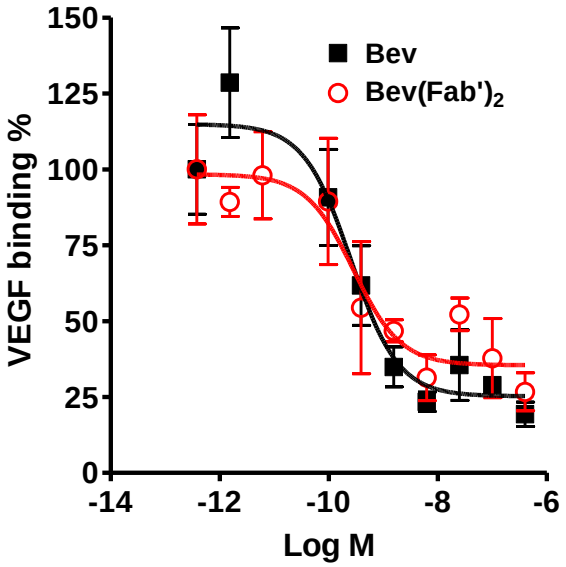

Supplemental Figure 1. Inhibition of ^{125}I-bevacizumab binding to VEGF-coated ELISA plates by bevacizumab (Bev) and BevF(ab')$_2$. The IC_{50} values for bevacizumab and BevF(ab')$_2$ were calculated to be (2.57 ± 0.19) ×10^{-10} and (2.84 ± 0.33) ×10^{-10} M, respectively (n = 4, means ± SD).

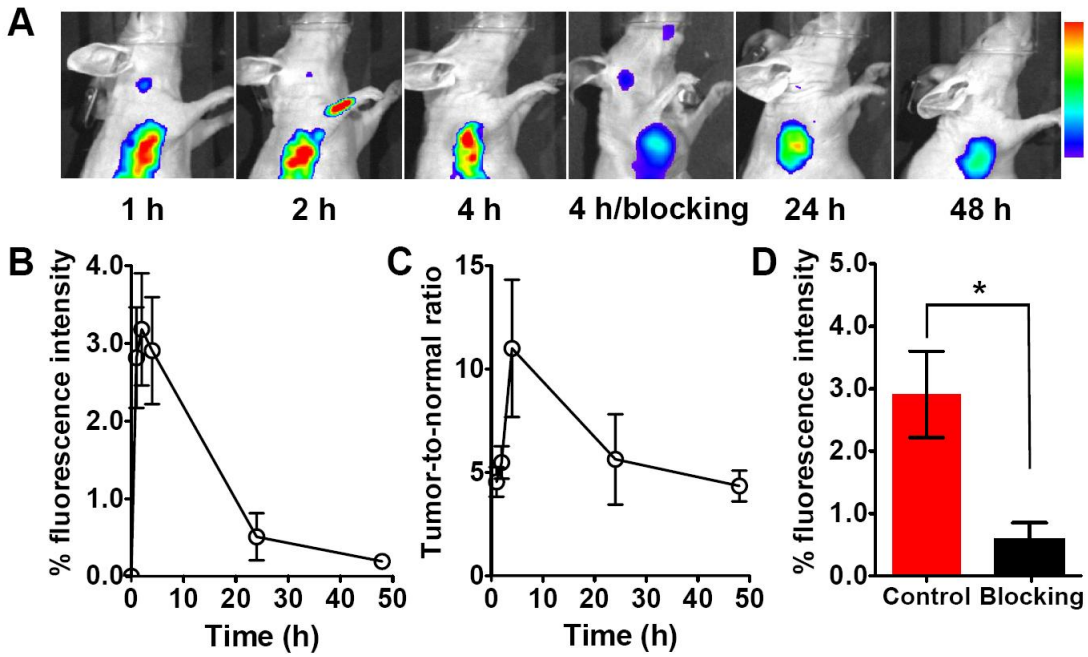

Supplemental Figure 2. (A) In vivo optical imaging of A549 tumor-bearing mice at 1, 2, 4 (with or without bevacizumab blocking), 24, and 48 h after intravenous injection of 0.5 nmol Dye-BevF(ab')$_2$. (B) Quantification and kinetics of in vivo tumor targeting characteristics of Dye-BevF(ab')$_2$ in A549 tumor-bearing mice. (C) The tumor contrast (tumor-to-normal tissue ratio) as a function of time after intravenous injection of Dye-BevF(ab')$_2$ in A549 tumor model. (D) Quantified A549 tumor uptake at 4 h after intravenous injection of 0.5 nmol Dye-BevF(ab')$_2$ (without or with bevacizumab as a blocking agent) (n = 5, means ± SD; *: $P < 0.05$).

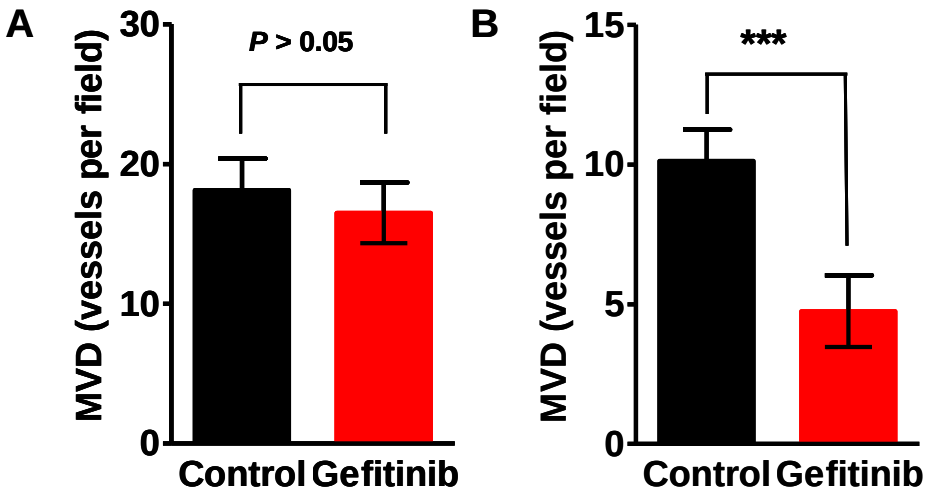

Supplemental Figure 3. Quantified microvascular density (MVD) in gefitinib-treated and control 22B (A) and A549 (B) tumors (n = 20, means ± SD; ***: $P < 0.001$).

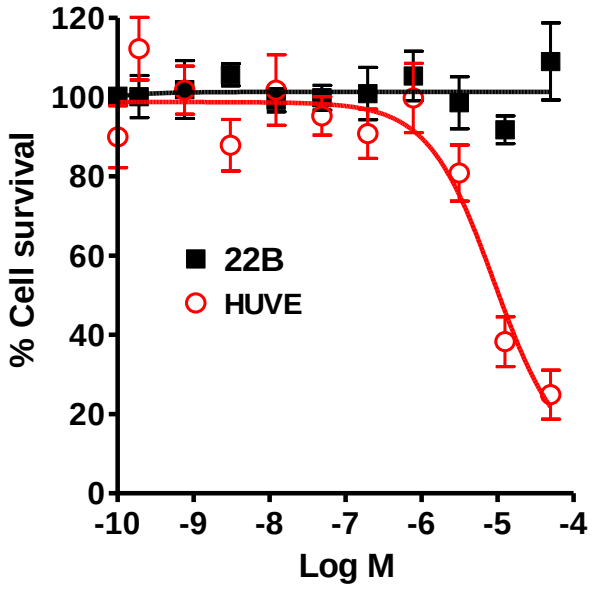

Supplemental Figure 4. Growth inhibitory effects of gefitinib on HUVE and 22B cells (n = 8, mean ± SD).